Zhou *et al. Fashion and Textiles* (2022) 9:3
https://doi.org/10.1186/s40691-021-00283-4

Fashion and Textiles

RESEARCH Open Access

The relevance of breast motions and gaits in running exercises

Jie Zhou[1], Qian Mao[1*], Jun Zhang[2*], Newman M. L. Lau[2] and Jianming Chen[3]

*Correspondence: 17802592059@163.com; alice.zj.zhang@connect.polyu.hk
[1] School of Apparel and Art Design, Xi'an Polytechnic University, No. 19 Jinhua South Road, Xi'an, Shaanxi, China
[2] School of Design, The Hong Kong Polytechnic University, Hung Hom, Kowloon, Hong Kong
Full list of author information is available at the end of the article

Abstract

The control of breast motions is a critical indicator to evaluate the comfort and function of sports bras. If the breast motions can be predicted based on the gait parameters detected by wearable sensors, it will more economical and convenient to evaluate the bras. Thirteen unmarried Chinese females with a breast cup of 75B were recruited in this study to investigate the regularity of breast motions and the relevance between breast motions and gaits during running exercises. The breast motion indicator is the distance alteration of breast regions. The gaits were described by the rotation angles of the hip, knee, ankle joints, and the foot height off the ground. Firstly, the Mann-Whitney U test and the Kruskal-Wallis H test were utilized to analyze the motion diversity among the eight breast regions. Then, the gray correlation analysis was applied to explore the relevance between breast motions and gaits. Finally, the back-propagation neural network, the genetic algorithm, and the particle swarm optimization algorithm were utilized to construct the prediction models for breast motions based on gait parameters. The results demonstrate that the same breast regions on the bilateral breasts and the different breast regions on the ipsilateral breasts present a significant motion diversity. There is a moderate correlation between breast motions and gait parameters, and the back-propagation neural network optimized by the particle swarm optimization algorithm performs better in breast motion prediction, which has a coefficient of determination of 84.58% and a mean absolute error of 0.2108.

Keywords: Breast motions, Gaits, Running exercises, Back-propagation neural network, Optimization algorithms

Introduction

The female breasts primarily consist of external skins and internal structures (fibro-adipose and fibro-glandular tissues) (McGhee & Steele, 2020a). The thickness and elasticity of human skins decrease as age increases (Coltman et al., 2017; Den Tonkelaar et al., 2004). Besides, the configuration of the internal structure is affected by age, race, weight, hormones, and so on (Boyd et al., 2009; Huang et al., 2011; Lee et al., 1997; McGhee & Steele, 2020a). Specifically, the proportion of fibro-glandular tissue decreases while the fibro-adipose percentage increases by the aging process (Boyd et al., 2009; Huang et al., 2011; Lee et al., 1997). It was well-documented that the lack of breast support causes women to experience frequent breast pain during exercises (McGhee et al., 2007).

Hence, enough external support for breasts is necessary for women. However, according to the relevant surveys, 56% of females have experienced breast pain during exercises (Lorentzen & Lawson, 1987). The larger breasts are, the more painful the sensations that women feel. As bras providing with sufficient support are capable of reducing the excessive breast motions and even the perceived pains (Scurr et al., 2011), numerous studies have been done to observe the characteristics of the breast motions among different exercises to improve bra support (McGhee et al., 2013; Scurr et al., 2011; Zhou et al., 2012).

Due to a lack of advanced measurement techniques and awareness of breast motions, Gerhlsen and Albohm only investigated the absolute displacement of the breasts in the coronal plane (Gehlsen & Albohm, 1980). The displacement trajectory tended to a figure-of-eight pattern. With the development of motion capture techniques, researchers began to investigate the breast motions in three dimensions (Scurr et al., 2009; Wood et al., 2012; Zhou et al., 2012). Awareness of the relative property of breast motions in three dimensions also improves the development of a series of new coordinate systems and breast motion indicators (Milligan et al., 2015; Scurr et al., 2009; Zhou et al., 2009, 2012). Zhou et. al. (2012) established a breast coordinate system based on four torso markers to eliminate the torso motions from the breast motions. The motions of six breast points presented a butterfly shape. In addition, it was speculated that relative breast motions were caused by the breast deformations and the stretching or contracting behavior of pectoralis major muscle (McGhee & Steele, 2020a). Lots of numerical models have also been constructed to study the constitutive material coefficients for breast tissues. Cai et. al. (2018) established a mass-spring-damper model for simulating breast motions. The abstract model verified the diversity of breast motions among difference regions. Most of the existing researches focused on a series of point motion for the breasts, whereas the point motion cannot effectively reflect the deformation of the breasts. Thus, this study aims to investigate the extension and contraction of the breast surface based on the distance alterations of different breast regions. This awareness may help bra designers to improve the bra support in terms of the bra structure and fabric elasticity.

During exercises, breast motions are influenced by the torso driving force, the viscoelastic mechanical properties, and the bra's supporting ability (Haake & Scurr, 2010). Previous literature reported that the females may change their body posture to reduce the breast motions and pains (White et al., 2009). Milligan et. al. (2015) compared the motion patterns of human torso, pelvis, and upper arm during a 5 km running exercise. The results demonstrated that the high supportive bras perform better in terms of decreasing arm extension than the lower one. In addition, the breast displacements increase as the stride length exaggerates (Eden et al., 1992). Meanwhile, the rhythm of running or walking for females wearing sports bras was significantly lower than those baring breasts (Li et al., 2018). There might be a relationship between breast motions and gait patterns. Such experimental motion analyses are very restricted by their complicated setup, large workload of data cleaning and processing. If the breast motions can be predicted based on a wider breadth of gait patterns, the bra's support will be evaluated, thus more information on bra performance is bale to be provided efficiently. Besides, by deeper perception of how lower limb movements influence breast motions, the bra

designers can optimize the application-centered bra design. Therefore, it is necessary to explore the patterns of breast motions under different gaits. The results will provide a scientific basis for the design of sports bras.

The back-propagation (BP) neural network is a kind of feed-forward neural network with a simple structure and wide applications. The neural network can approximate any continuous function and square productive function with arbitrary accuracy (Zhou & Ma, 2019). Thus, this method has been widely applied to deal with non-linear problems such as girdle pressure prediction (Zhou & Ma, 2020), fabric surface detection (Jin et al., 2020), and flow stress prediction (Ding et al., 2020). However, the BP neural network has great defects in threshold and weight initialization. To avoid the BP neural network falling into the local optimum, researchers (Ding et al., 2020; Zhang & Guo, 2019; Zhou & Ma, 2020) usually adopted the genetic algorithm (GA) and the particle swarm optimization (PSO) to optimize the BP neural network. The GA is a computational model of biological evolution. This method searches for the optimal solution by simulating the natural evolutionary process (Zhang & Guo, 2019). The PSO is a kind of optimization algorithm based on iteration, and it can search the optimal threshold and weight of the BP neural network in a large space (Ding et al., 2020).

The distance alteration of the breast regions was applied to investigate the characteristics and diversities of breast motions in this study to address the above mentioned issues. Meanwhile, four gait parameters, including the hip, the knee, the ankle joint motion angles, and the foot height off the ground, were utilized to explore the correlation between breast motions and gaits. Moreover, the BP, the back-propagation neural network optimized by the genetic algorithm (GA-BP), and the back-propagation neural network optimized by the particle swarm optimization (PSO-BP) were adopted to establish the prediction models for breast motions based on gait parameters. Therefore, the following are the research questions to be answered. (1) What characteristics do the breast motions present in different parts during running exercise, and whether the motion differs in various breast regions? (2) What kind of correlation exists between breast motions and gait parameters? (3) If there is a desirable correlation between breast motions and gaits, the BP neural network optimized by the GA and PSO algorithms will be utilized to forecast breast motions. The mean absolute error and the coefficient of determination were determined to evaluate the accuracy of the models.

Methods

Subjects

Fifteen young Chinese females were recruited for measuring their breast sizes. B-cup breasts are the most prevalent in unmarried Chinese females (Liang et al., 2007; Mao et al., 2020). Thus, thirteen subjects with B-cup were chosen and two females with other cups were excluded in this study. All subjects were given consent form and had no pregnancy or breast disease experience. Ethical approval was obtained from the ethics committee of Xi'an Polytechnic University. The essential physical characteristics of the subjects are shown in Table 1.

Table 1 The essential physical characteristics of the subjects

Physical characteristics	Mean ± SD	Physical characteristics	Mean ± SD
Age (years)	21.50 ± 1.12	Waist circumference (cm)	65.87 ± 4.33
Height (cm)	159.92 ± 4.69	Buttocks circumference (cm)	88.42 ± 3.26
BMI (kg/m^2)	19.53 ± 0.51	Bi-acromial breadth (cm)	36.76 ± 1.42
Arm length (cm)	51.87 ± 2.73	Bust breadth (cm)	28.09 ± 1.31
Neck circumference (cm)	31.23 ± 1.69	Waist breadth (cm)	24.18 ± 1.86
Bust circumference (cm)	85.60 ± 1.69	Buttocks breadth (cm)	33.35 ± 1.21

Table 2 The definitions of the marker positions

Marker	Definition
Left/right bust points (L_0/R_0)	The nipple points of the left/right breast
Left/right breast lateral midpoints (L_1/R_1)	The midpoints of the left/right breast nipple points and the lateral edge points
Left/right breast upper midpoints (L_2/R_2)	The midpoints of the left/right breast nipple points and the upper edge points
Left/right breast medial midpoints (L_3/R_3)	The midpoints of the left/right breast nipple points and the medial edge points
Left/right breast lower midpoints (L_4/R_4)	The midpoints of the left/right breast nipple points and the lower edge points
Left/right hip joint points (LI_1/RI_1)	The anterior superior iliac spine points of the left/right leg
Left/right knee joint points (LI_2/RI_2)	The lateral epicondyle points of the left/right leg femur
Left/right ankle joint points (LI_3/RI_3)	The external ankle points of the left/right leg fibula

Data capture

The experiment was carried out in a quiet, windless laboratory, with 25 ± 2 °C and relative humidity of 65 ± 3%. The subjects were asked to run on a treadmill (slope of 0°) at 7 km/h with nude upper body and tight-fitting athletic pants. Sixteen reflective markers were pasted on their bodies. The three-dimensional (3D) coordinates of the reflective markers were collected at 120 Hz frequency by a Vicon 612 (Oxford Metric, UK) motion analysis system. The system is comprised of 12 M-series cameras and its mean residual is 0.605 mm.

The positions of ten breast markers and six leg markers were defined to explore breast motions and gaits (Ren et al., 2015; Wang et al., 2019; Zhou et al., 2012). The definitions of the marker positions are shown in Table 2.

Firstly, the subjects carried out a 3-min exercise on the treadmill following their running habits. Then, the subjects were asked to stand naturally and a professional technician pasted the reflective markers on their body based on the Table 2. Finally, the Vicon workstation software (v5.2.9) was utilized to track and record the 3D coordinates of the reflective markers during natural standing and running. No less than ten seconds of natural standing and one minute of running were recorded for three times. The data without missing values for each marker at the same time were adopted for this study.

Data processing

The gait cycles were divided according to the vertical coordinate of the Ll_3. A complete gait cycle was defined as a nadir to another nadir in the vertical coordinate. Three complete consecutive gait cycles were extracted for each subject. As a result, a total of 39 gait cycles were obtained to analyze the breast motions and gaits.

Breast motion parameters

The displacement, velocity, and acceleration were utilized to investigate the breast point's motions (Scurr et al., 2010; Zhou et al., 2009), however, the motions of the breast areas were ignored in these reports. The distance alteration of the breast regions (Δd) was applied in this study to explore the extension and contraction of the breast surface during exercises as shown in Eq. (1). The eight breast regions are divided as shown in Fig. 1.

$$\Delta d_{ij} = d_{ij}(t) - d'_{ij}, \tag{1}$$

where $d_{ij}(t)$ is the euclidean distance between breast point i and j at moment t, d'_{ij} is the mean euclidean distance between breast point i and j in a natural standing state.

To improve the quality of the data, the normality and outliers of Δd were checked. Measurements of Δd that smaller than the first quartile—(1.5 × interquartile range) or larger than the third quartile + (1.5 × interquartile range) were considered as outliers (Shen et al., 2018). The change of the data before and after deleting the abnormal values is shown in Fig. 2.

As shown in Fig. 2, the Δd data maintain the same distribution after eliminating the outliers. Compared with the right breasts, there are more abnormal values in the left breasts, especially in the d_{01} regions.

Gait parameters

The vertical displacement of the breasts is closely related to foot strikes during running (McGhee & Steele, 2020b). Therefore, the foot height off the ground (Δh), the hip, the knee, and the ankle joint rotation angles (α, γ, β) were determined as the gait parameters in this study. And the illustration of four parameters (left leg) is shown in Fig. 3.

The Ll_3' denotes the coordinates of the ankle joint points in a natural standing state, and the four parameters were calculated in Eqs. (2) and (3).

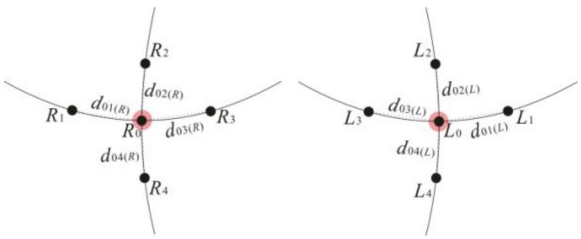

Fig. 1 The breast regions

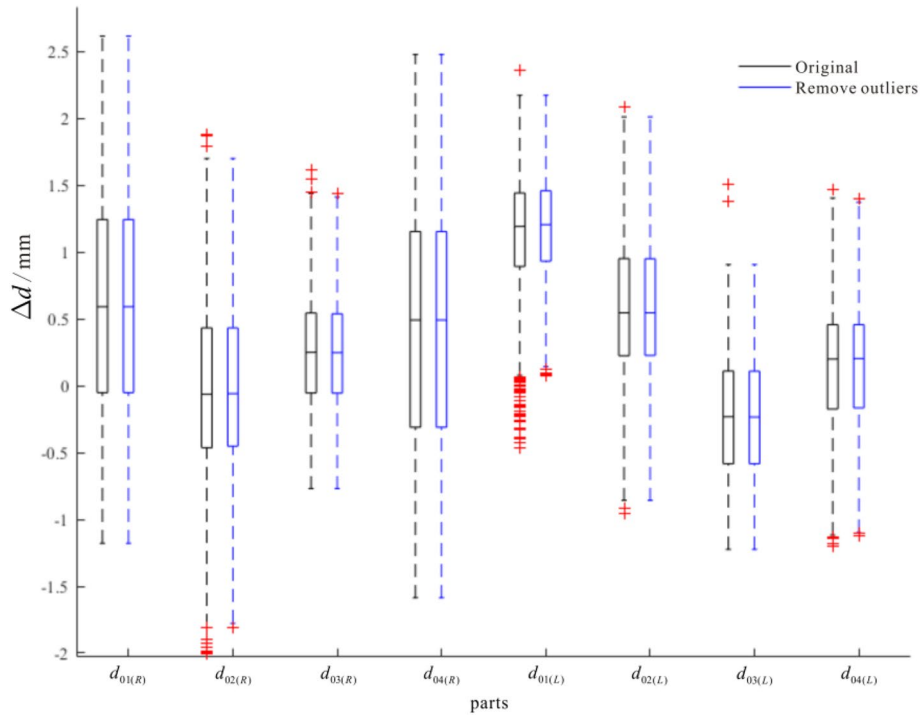

Fig. 2 The outliers of the Δd

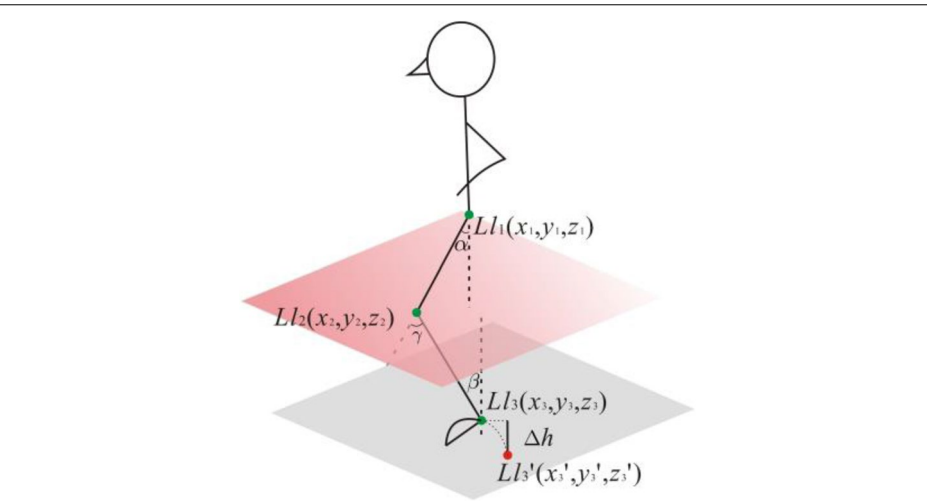

Fig. 3 Gait parameters (left leg)

$$\begin{aligned} a &= \sqrt{(x_1 - x_2)^2 + (y_1 - y_2)^2 + (z_1 - z_2)^2} \\ b &= \sqrt{(x_1 - x_3)^2 + (y_1 - y_3)^2 + (z_1 - z_3)^2} \\ c &= \sqrt{(x_2 - x_3)^2 + (y_2 - y_3)^2 + (z_2 - z_3)^2} \end{aligned} \tag{2}$$

where a is the euclidean distance between Ll_1 and Ll_2, b is the euclidean distance between Ll_1 and Ll_3, and c is the euclidean distance between Ll_2 and Ll_3.

$$\alpha = \arccos \frac{|y_1 - y_2|}{a},\ \beta = \arccos \frac{|y_3 - y_2|}{c},\ \gamma = 180^{\circ} - \arccos \frac{a^2 + c^2 - b^2}{2ac},\ \Delta h = z_3 - z_3'. \tag{3}$$

Prediction models for breast motions

Numerous researches for breast motions are based only on running and they lack other exercises (McGhee & Steele, 2020a). With the development of wearable sensors, it is convenient and easy to detect the gaits outdoor (Prakash et al., 2018). If the breast motions are able to be predicted by gait parameters, the bra comfort and support will be evaluated in any situation. The BP neural network has excellent nonlinear mapping capability (Zhou & Ma, 2019), while the GA and the PSO algorithms can effectively optimize the BP neural network. The BP, the GA-BP, and the PSO-BP algorithm were applied in this study to establish the prediction models for breast motions.

The principle for BP neural network

Matlab 2017B version (MathWorks, USA) was utilized in this study to construct a BP neural network reflecting the nonlinear mapping relationship between breast motion indicators and gait parameters. Meanwhile, the gray correlation degree was adopted to calculate the weight of gait parameters (ξ) related to Δd. The ξ was calculated in Eq. (4).

$$\xi_{ij} = \frac{\delta_{ij}}{\sum_{i=1}^{8} \delta_{ij}}, \tag{4}$$

where i and j are the gait parameters and the Δd, respectively. δ_{ij} denotes the gray correlation degree between i and j. The results of ξ are shown in Table 3.

There were nine nodes in the input layer, including eight weighted gait parameters and breast region numbers (the breast regions $d_{01(R)}$, $d_{02(R)}$, $d_{03(R)}$, $d_{04(R)}$, $d_{01(L)}$, $d_{02(L)}$, $d_{03(L)}$, $d_{04(L)}$ were set as 1, 2, 3, 4, 5, 6, 7, 8, respectively). The output layer was the value of Δd. The optimal number of hidden layer nodes was mainly obtained by the trial-and-error method and the mean absolute error (*MAE*) was utilized as the evaluation index. The number was first set to five and then gradually increased to 50. When the number was 35, the *MAE* reached the smallest and the BP neural network performed better. Thus,

Table 3 Weights of gait parameters related to Δd

Gait parameters	$d_{01(R)}$	$d_{02(R)}$	$d_{03(R)}$	$d_{04(R)}$	$d_{01(L)}$	$d_{02(L)}$	$d_{03(L)}$	$d_{04(L)}$
$\alpha_{(L)}$	0.13	0.12	0.12	0.12	0.13	0.13	0.14	0.13
$\beta_{(L)}$	0.12	0.12	0.12	0.12	0.12	0.12	0.11	0.12
$\gamma_{(L)}$	0.12	0.13	0.13	0.13	0.12	0.12	0.12	0.12
$\Delta h_{(L)}$	0.12	0.12	0.13	0.12	0.13	0.13	0.12	0.13
$\alpha_{(R)}$	0.13	0.13	0.13	0.13	0.13	0.13	0.13	0.13
$\beta_{(R)}$	0.13	0.13	0.13	0.13	0.12	0.12	0.12	0.12
$\gamma_{(R)}$	0.12	0.12	0.12	0.12	0.12	0.12	0.12	0.12
$\Delta h_{(R)}$	0.13	0.13	0.13	0.13	0.12	0.12	0.12	0.12

the topology of the BP neural network was finally determined to be 9-35-1, as shown in Fig. 4.

There are 21,827 sets of data in the sample set. In this study, 21,500 sets of data were randomly selected as the training set of the models, and the rest were the test set (327). In order to accelerate the convergence of the BP neural network, the input and output data were normalized to the range of $[-1, 1]$ based on the Eq. (5).

$$y = \frac{(y_{\max} - y_{\min})(x - x_{\min})}{x_{\max} - x_{\min}} + y_{\min}, \tag{5}$$

where x and y represent the original data and normalized data, respectively.

The transfer functions of the BP neural network include linear function (purelin) and sigmoid function (logsig and tansig). The output of the purelin function is an arbitrary value. The logsig function maps the neuron from $(-\infty, +\infty)$ to $(0, 1)$, while the tansig function maps the neuron from $(-\infty, +\infty)$ to $(-1, 1)$. Therefore, the tansig and the purelin were determined as the transfer function of the hidden and output layer, respectively. Meanwhile, the training function of the models is trainlm in this study. The maximum number of iteration steps, the training target, the learning rate, and the number of verification failures were set as 1000, 0.001, 0.01, and 6, respectively.

In order to avoid the BP neural network falling into the local optimum, we applied the GA and PSO algorithms to optimize the initial weights and thresholds for the BP neural network. Meanwhile, the topology of the BP neural network was maintained.

The principle for GA-BP neural network

The principle for the GA algorithm is to utilize individuals to represent the initial weights and thresholds of the BP neural network. Meanwhile, the GA algorithm takes the prediction error of the initial neural network as an individual fitness value to find the optimal initial parameters (Ding et al., 2020). The parameters of the GA algorithm were initialized firstly in this study. After repeated tests, the population size, the maximum number of iteration, the crossover probability, and the mutation probability were determined to be 8, 50, 0.4, and 0.2, respectively. Then, the real coding was utilized for individual coding, and the length of coding was calculated in Eq. (6).

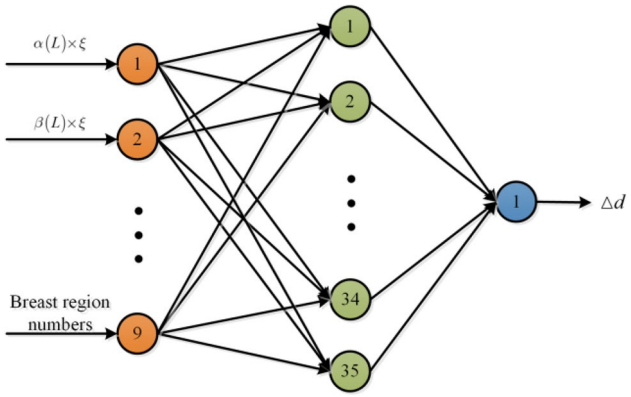

Fig. 4 The topology of BP neural network

$$S = S_1S_2 + S_1S_3 + S_1 + S_3, \tag{6}$$

where S_1 is the number of hidden layer nodes, S_2 and S_3 are the number of the input layer and output layer nodes, respectively.

The next step is to select the fitness function. The individual was utilized to represent the initial weights and thresholds of the neural network, and the absolute error of the neural network initialized by the individual was adopted as the fitness value F as shown in Eq. (7).

$$F = k\left(\sum_{i=1}^{S_3}\left|y_i - o_i\right|\right), \tag{7}$$

where k is the coefficient, y_i and o_i are the expected output and the predictive output, respectively.

The fitness ratio method was adopted to carry out the selection operation of the genetic algorithm. If an individual is set as X_i and its fitness is F_i, the selection probability is P_i as shown in Eq. (8).

$$P_i = \frac{F_i}{\sum_{i=1}^{S} F_i}. \tag{8}$$

The process of gene recombination is known as cross operation. The cross mode of the k chromosome a_k and the l chromosome a_l at the j position are shown in Eq. (9).

$$\begin{cases} a_{kj} = a_{kj}(1-b) + a_{lj}b \\ a_{lj} = a_{lj}(1-b) + a_{kj}b \end{cases}, \tag{9}$$

where b is a random number between 0 and 1.

The j-th gene of the i-th individual is selected for mutation operation as shown in Eqs. (10) and (11).

$$a_{ij} = \begin{cases} a_{ij} + \left(a_{ij} - a_{\max}\right)f\left(g\right), & r > 0.5 \\ a_{ij} + \left(a_{\min} - a_{ij}\right)f\left(g\right), & r \le 0.5 \end{cases}, \tag{10}$$

$$f\left(g\right) = r_1\left(1 - \frac{g}{G_{\max}}\right)^2, \tag{11}$$

where $a_{\max}$ is the maximum value of a_{ij} and $a_{\min}$ is the minimum value of a_{ij}; g is the number of iterations; $G_{\max}$ is the maximum number of evolution; r_1 is a random number, and r is a random number between 0 and 1.

After the evolution of the GA algorithm, the optimal individuals were obtained. Finally, the prediction model was established by training the neural network. The specific process is shown in Fig. 5.

The principle for PSO-BP neural network

The PSO algorithm is a parallel random search algorithm, which performs global searches under individual fitness conditions. In this process, the speed and position

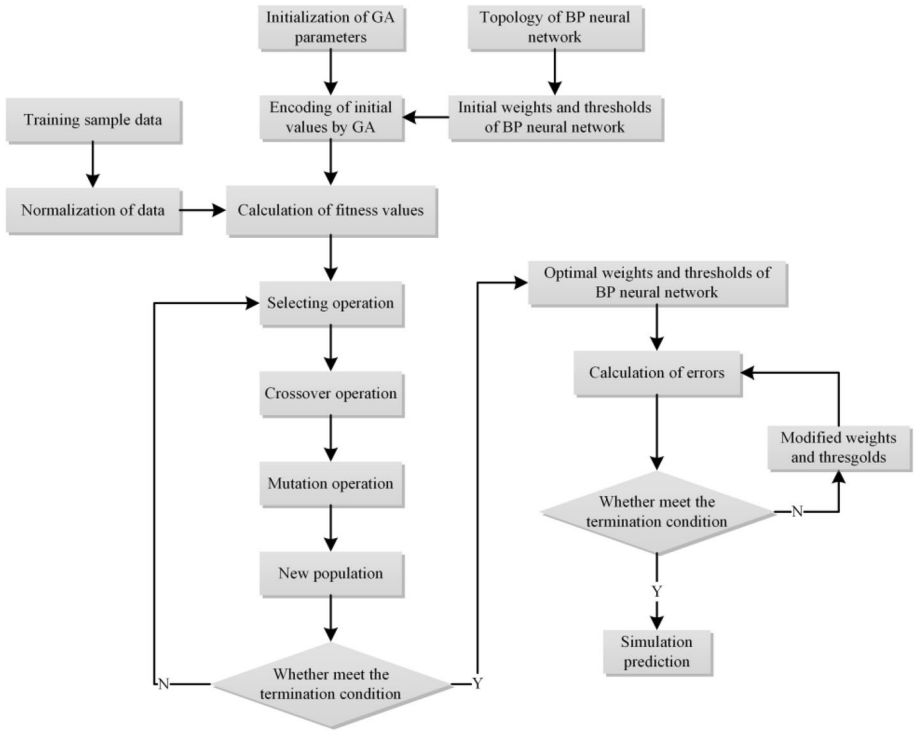

Fig. 5 The process of the GA-BP algorithm

of each particle are constantly updated to accurately approach the target within a short period (Ding et al., 2020). The PSO algorithm also requires population initialization like the GA algorithm, but it has no selection, crossover, and mutation operations. Herein, the population size and the maximum number of iterations were also determined as 8 and 50, respectively.

In the searching space, the PSO algorithm randomly initializes a group of particles. Each particle represents a potential optimal solution to the extreme value optimization problem. The fitness value of each particle is calculated according to the Eq. (7). The particle updates the individual position in the searching space by tracking the individual extreme value (Pbest) and the group extreme value (Gbest). In each iteration, the particle updates its speed and position through individual extreme value and group extreme value, as shown in Eq. (12).

$$\begin{cases} v_{ij}(t+1) = \omega v_{ij}(t) + c_1 r_2 \left[P_{best}(t) - x_{ij}(t)\right] + c_2 r_3 \left[G_{best}(t) - x_{ij}(t)\right] \\ x_{ij}(t+1) = x_{ij}(t) + v_{ij}(t+1) \end{cases}, \tag{12}$$

where v_{ij} represents the j-th dimension component of the i-th particle velocity. The particle velocity was limited between $[-1, 1]$ in this study. t is the current iteration number, and ω is the inertia weight, herein, its range was set in [0.4, 09]. c_1 and c_2 are acceleration constants, herein, $c_1 = c_2 = 1.5$; r_2 and r_3 are random numbers between 0 and 1; x_{ij} is the j-th dimension component of the position of particle i. The motion range of the particles was set in $[-5, 5]$.

At the end of the PSO algorithm, the optimal initial weights and thresholds were output, and the prediction model was acquired by training the network. The specific process is shown in Fig. 6.

Results

Breast motions

Some reports have found that there is a significant difference between the left and right breasts in terms of morphology and kinematics (Pei et al., 2019; Ren et al., 2016). The breast motions also exhibit considerable variability in different breast parts (Mason et al., 1999). The study aims to investigate the difference of breast extension and contraction between breast regions, SPSS 20.0 version (IBM, USA) was applied for the statistical analysis of Δd. Since the Δd were detected to be non-parametric data by the test for normal distribution, the Mann–Whitney U test was applied to analyze the motion diversity between the same regions on the bilateral breasts. Meanwhile, the Kruskal–Wallis H test was utilized to analyze the motion difference between different regions (d_{01}, d_{02}, d_{03}, d_{04}) on the ipsilateral breasts. All significance levels were predetermined at $p \leq 0.05$. The results are shown in Table 4.

As for the Δd, the positive and negative values represent the extension and contraction of breast regions, respectively. Combined with the Δd distribution in Fig. 2, most breast regions present both extension and contraction, except for the $d_{01(L)}$ region. According

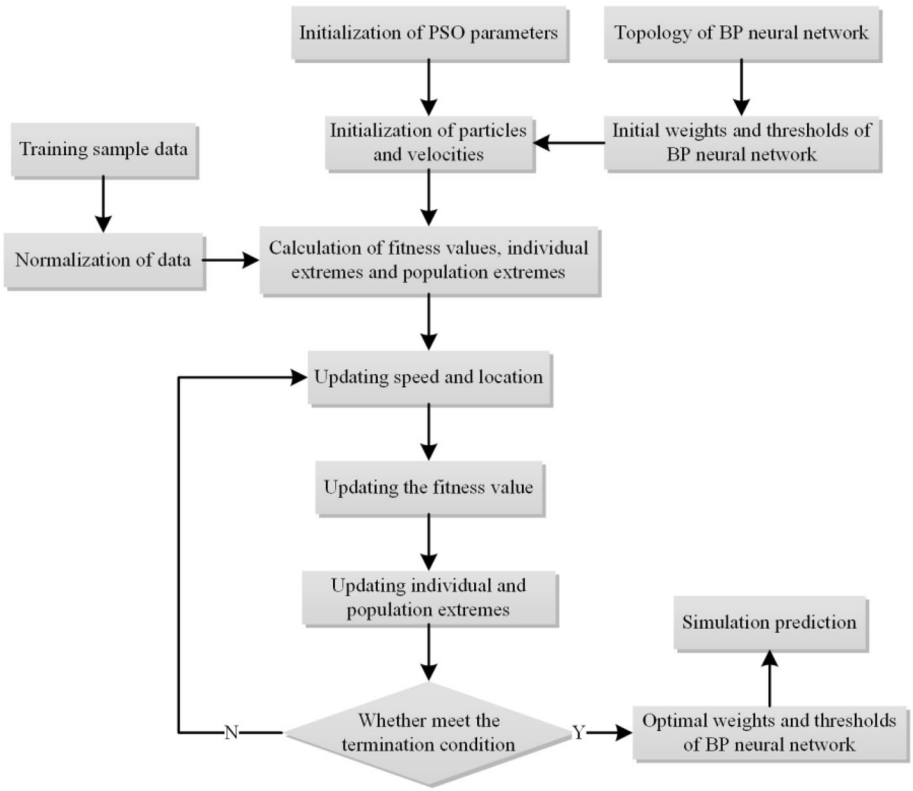

Fig. 6 The process of the PSO-BP algorithm

Table 4 Statistical characteristics of Δd (unit: mm)

Breast region	d_{01}		d_{02}		d_{03}		d_{04}	
	L	R	L	R	L	R	L	R
Min	0.08	− 1.18	− 0.86	− 1.81	− 1.22	− 0.77	− 1.12	− 1.59
Max	2.17	2.61	2.01	1.70	0.90	1.44	1.40	2.48
Range	2.09	3.79	2.87	3.51	2.12	2.21	2.52	4.07
Mean	1.18	0.61	0.58	− 0.01	− 0.23	0.26	0.14	0.42
SD	0.40*#	0.80*#	0.56*#	0.69*#	0.43*#	0.42*#	0.48*#	0.94*#

*Indicates a significant difference between the same regions on bilateral breasts (left and right breast)

# Indicates a significant difference between the different regions (d_{01}, d_{02}, d_{03}, d_{04}) on ipsilateral breasts

to the average values, the motion pattern of the $d_{01(L)}$, the $d_{01(R)}$, the $d_{02(L)}$, the $d_{03(R)}$, the $d_{04(L)}$, and the $d_{04(R)}$ regions are mainly extension, while the $d_{02(R)}$ and $d_{03(L)}$ regions take contraction as the primary motion. In the d_{01} and d_{02} areas, the breast motions are more distinct in the left than in the right, and the reverse phenomenon occurs in the d_{03} and d_{04} breast regions. The phenomenon demonstrates that the motions of breast regions vary between the left and right breasts. As for the upper and outer breast regions, the motions are more intense in the left breasts, whereas the lower and inner breast regions move more intensely in the right breasts.

In terms of the range values, the four regions on the right breasts have a wider range of stretch than the left breasts, and the maximum value (4.07 mm) occurs in the $d_{04(R)}$. The result indicates that the breast motions are more active in the right breasts. The squared deviation (SD) indicates the dispersion degree of the breast motion indicators. Except for the d_{03} areas where the SD values are similar in bilateral breasts, the other regions have different SD values between the right breasts and the left breasts. The SD values in the right breast regions were much greater than those in the left breasts. The result indicates that the right breast motions are more scattered and irregular than the left breasts. As shown in Table 4, there are significant motion differences in the same regions on the bilateral breasts or the different regions on the ipsilateral breasts according to the two non-parametric tests. Numerous reports have verified the morphological asymmetry of bilateral breasts (Losken et al., 2005; Pei et al., 2019). Based on the investigation of local breast motions, the asymmetry of bilateral breast motions was found in this study. Therefore, the bra producers and designers are advised to improve the bra comfort and support based on the differences in both breast morphology and motions.

Relevance of breast motions and gaits

Due to the influence of trunk displacements, breast motions also present a periodic pattern (McGhee et al. 2013). Besides, the intensity of breast motions may lead to gait changes during exercises (Eden et al., 1992; Li et al., 2018). Thus, whether a correlation exists between breast motions and gaits is speculated. The mean values of parameters were calculated for correlation analysis. The duration of three cycles varies with individual subjects for the unavoidable changes in the arm swing amplitude (Zhou et al., 2012). Therefore, the gait cycles were reshaped by the reshape function in Pandas of Python. The maximum duration of cycles was determined as the new

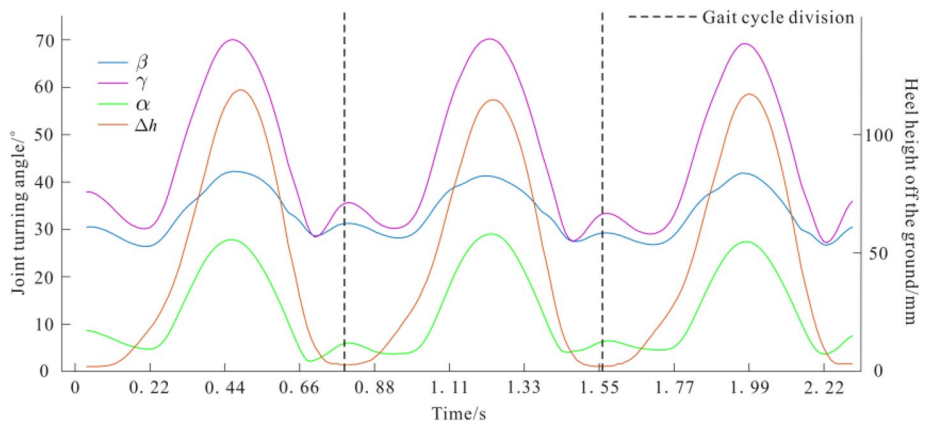

Fig. 7 Variations of gait parameters with time (left leg)

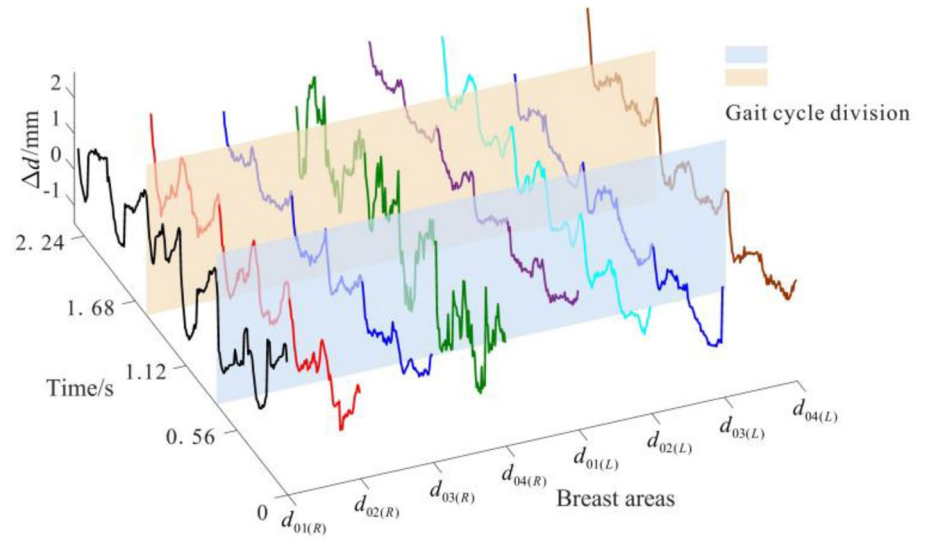

Fig. 8 Variations of Δd with time

duration, so the linear interpolation method was applied to increase the samples. The average gait and breast motion parameters for 13 subjects over time are shown in Figs. 7 and 8, respectively.

As shown in Fig. 7, the curve of Δh with time is similar to the sine curve. The wave shapes of the lower limb rotation angles including the β, the γ, and the α are similar to each other, and the curves all present a 'W' shape with a single peak and two troughs. Although the Δh curve is different from three other gait parameters, the four curves all present a stable periodic structure. Their peaks and the troughs also exhibit a period of synchronicity. On top of this, the hip rotation angle α has the smallest value, and the ankle rotation angle β has the relatively minimum range of change (26.89°). The knee rotation angle γ has the largest value and the maximum change range (42.98°). The result reveals that the knee rotation joint has the maximum motion amplitude while the ankle rotation joint has the minimum motion amplitude.

Figure 8 shows that the Δd exhibits a continuous periodicity with time and the curves approximately present a periodic 'V' shape. There are two breast motion cycles in a gait cycle according to the gait cycle division. Thus, the period of breast motions is half of the gaits. The phenomenon demonstrates that breast motions are more frequent than trunk movements. The event is perhaps a critical factor to cause breast pain. Compared to the gait parameters, the Δd values include more noise and present a relatively large fluctuation. As a result, the main features of breast motions are obscured and it may be detrimental to the correlation analysis between breast motion and gait. In order to reduce the noise of Δd, the wavelet threshold de-noising method was applied in this study to process the breast motion indicators. The result is shown in Fig. 8. In a single gait cycle, the patterns of the β, the γ, and the α are similar to the wave shape of the breast motion indicators. They all show a 'W' shape. Thus, the knee rotation angle γ (left leg) having the largest amplitude was determined to compare with the breast motions. The results are shown in Fig. 6. Meanwhile, the Mann–Whitney U test was applied to analyze the variability of two breast motion cycles in a gait cycle. The significance level was predetermined at $p \leq 0.05$.

According to Fig. 9, although there are differences in the peaks and troughs of Δd and γ, the curves both show a 'W' shape within the same gait cycle. For the knee rotation angle γ, the peaks are more bulging while the troughs are a little concave. Meanwhile, the peaks and troughs have similar extents in the breast motion curves. In terms of the appearance times of the wave peaks and troughs, the peaks of Δd for the $d_{03(R)}$, the $d_{01(L)}$, the $d_{02(L)}$, and the $d_{04(L)}$ regions are consistent to the γ, respectively. It is interesting to observe that the peaks of Δd for the $d_{01(R)}$, the $d_{04(R)}$, and the $d_{03(L)}$ regions lag behind the γ, while the crests of Δd for the $d_{02(R)}$ are ahead of the γ. The appearance times of troughs within a gait cycle show another characteristic. The first valley of Δd always lags behind the γ, whereas the second valley of Δd advances or synchronizes with the γ. The time lag of peaks and troughs may be due to the lack of bone and muscle in the breasts or the viscoelasticity variability between different breast parts (Cai et al., 2018; McGhee & Steele, 2020a).

Although the expansion and contraction of the breasts show a V-shaped cycle in general, there are some phenomena of 'rebound' in the wave troughs. The phenomena illustrate that breast motions have a non-linear and complex character. The breast motion

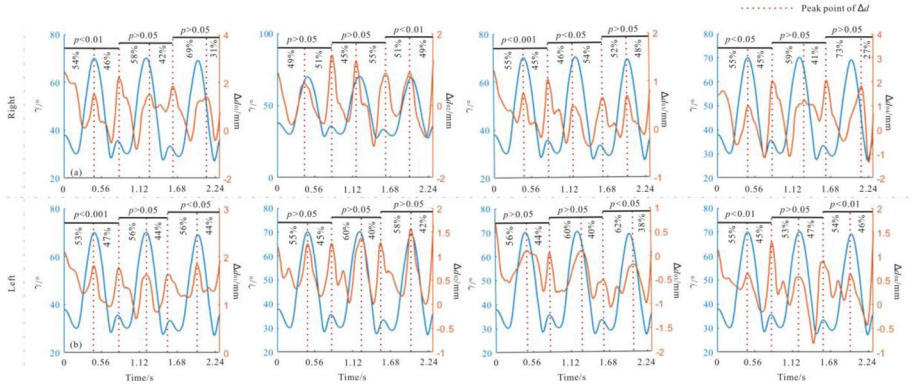

Fig. 9 Variations of Δd and γ with time

curves were divided into two cycles in a gait cycle, and the proportion of each breast motion cycle (breast motion cycle/gait cycle×100%) was calculated. The results find that the first cycle of Δd is longer than the second cycle except for the $d_{02(R)}$ and the $d_{03(R)}$ regions. According to the results of the Mann–Whitney U test, breast regions have significant differences between the two cycles except for $d_{02(L)}$ and more significant differences exist for $d_{03(R)}$, $d_{01(L),}$ and $d_{04(L)}$ regions. The results mean that the breast motions are more intense and complex than the gaits and they lead to the poor stability of the Δd curves.

Gray relational analysis is a quantitative method to describe and compare the developmental dynamics of a system. The larger the gray correlation degree (δ), the more similar the variation trend of the two variables, and vice versa (Xiao, 1997). The strength of the correlation is defined as weak $\delta \leq 0.49$, moderate $\delta \geq 0.50$ to $\delta \leq 0.74$, and strong $\delta \geq 0.75$ (Bridgman et al., 2010). The gray correlation degrees between parameters are shown in Fig. 10.

From Fig. 10, the gait parameters have the smallest δ value between the left and right leg, and the maximum value among them is only 0.62. However, the δ values between the ipsilateral gait parameters are all above 0.75. The gray correlation degree between α and

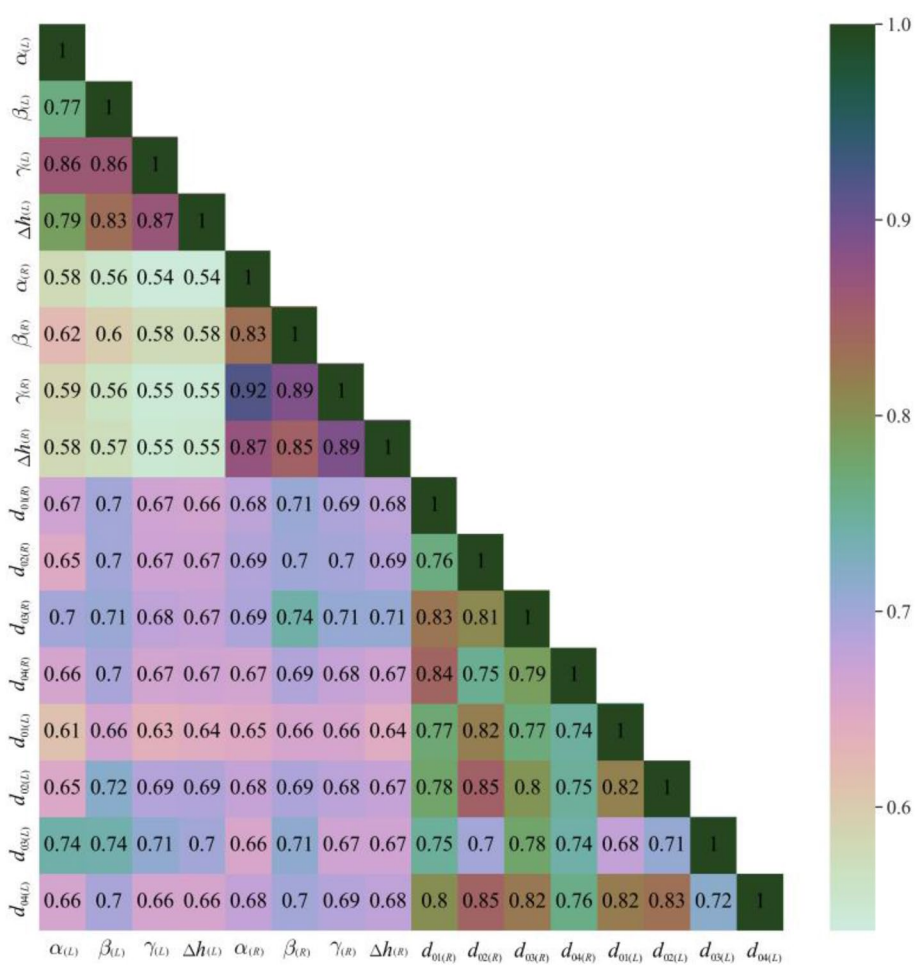

Fig. 10 Grey correlation degrees between breast motion indicators and gait parameters

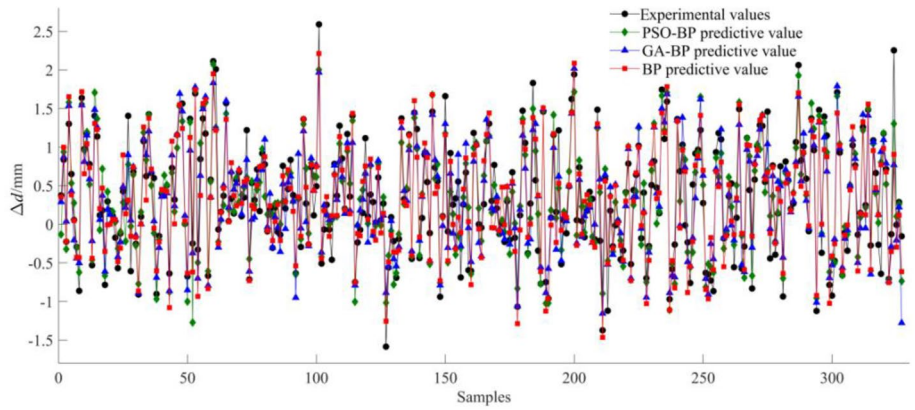

Fig. 11 The predictive results of the neural network models

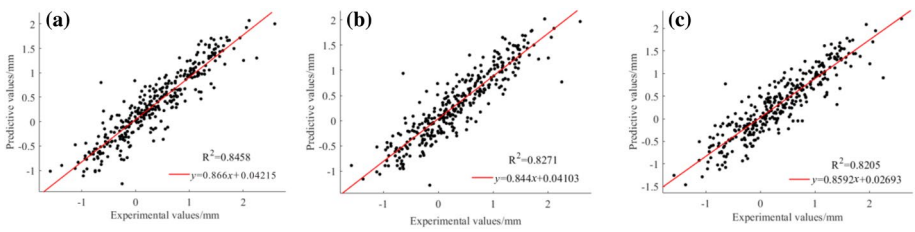

Fig. 12 The R^2 between experimental and predictive values: **a** PSO-BP, **b** GA-BP, **c** BP

γ for the right leg reached the maximum (0.92). Moderate δ values are observed between the breast motion indicators, with a minimum value of 0.68. The δ values between $d_{04(L)}$ and other breast regions are the highest, while the gray correlation degree between $d_{03(L)}$, $d_{04(R)}$ and other breast regions are the lowest. The result indicates that the $d_{03(L)}$ and $d_{04(R)}$ areas have more complex and irregular motions. As the δ values between gait parameters and breast motion indicators are in the range of [0.6, 0.75], there is a moderate correlation between these two types of parameters. Therefore, the prediction models for breast motions based on gait parameters can be established in this study.

Forecast of breast motions

To compare the accuracy of the PSO-BP, the GA-BP, and the BP algorithms, the input and output data of the models were set up consistently in this study. The predictive values of the test set were output after training the three prediction models for breast motions. The predictive values and the experimental values of Δd are shown in Fig. 11.

Figure 11 shows that the values of Δd predicted by the PSO-BP, the GA-BP, and the BP neural network models differ lightly from the experimental data. Thus, the breast motion indicators in this study can be effectively predicted by the above three models based on the gait parameters. To quantify the performance of the models, we adopted the coefficient of determination (R^2) and the *MAE* to evaluate the prediction accuracy of the algorithms, as shown in Eqs. (13) and (14). The results are shown in Fig. 12 and Table 5, respectively.

Table 5 The *MAE* of PSO-BP, GA-BP, and BP models

Δd	PSO-BP	GA-BP	BP
$d_{01(R)}$	0.1682	0.1888	0.1179
$d_{02(R)}$	**0.2330**	**0.2391**	**0.2316**
$d_{03(R)}$	0.1406	0.132	0.1354
$d_{04(R)}$	**0.2234**	**0.2335**	**0.2429**
$d_{01(L)}$	0.1251	0.1309	0.1465
$d_{02(L)}$	0.1269	0.145	0.1501
$d_{03(L)}$	0.1407	0.1549	0.1972
$d_{04(L)}$	0.1429	0.188	0.1813
Overall	0.2108	0.2289	0.2371

The bold values are the top 20% of the MAE values

$$R^2 = 1 - \frac{\sum_{i=1}^{m} \left(\Delta d^{(i)} - \Delta d'^{(i)}\right)^2}{\sum_{i=1}^{m} \left(\Delta d'^{(i)} - \overline{\Delta d'}\right)^2}, \tag{13}$$

$$MAE = \frac{1}{m} \sum_{i=1}^{m} \left|\Delta d^{(i)} - \Delta d'^{(i)}\right|, \tag{14}$$

where Δd and $\Delta d'$ are the experimental and predictive value of the models respectively; $\overline{\Delta d'}$ is the average of the predictive values, and m indicates the sample size of the test set.

Figure 12 shows that the R^2 of the PSO-BP, the GA-BP, and the BP neural network models reaches more than 80%. The R^2 of the GA-BP and the BP neural network models are similar to each other, while the R^2 of the PSO-BP model has the maximum value of 84.58%. The result indicates that these three neural network models have the ability to predict the breast motions, and the PSO-BP model is more suitable for breast motion prediction in this study.

As shown in Table 5, the overall *MAE* of the PSO-BP model is 0.2108, which is 11% lower than that of the BP neural network. Meanwhile, the overall *MAE* of the GA-BP model is 0.2289, which is 3% lower than that of the BP neural network. The phenomenon indicates that both the PSO and GA algorithms have the ability to improve the prediction accuracy of the BP neural network for breast motions. The PSO-BP model has the best prediction accuracy. Among the three prediction models for breast motions, the *MAE* of $d_{02(R)}$ and $d_{04(R)}$ are larger than other breast regions. The result demonstrates that the motion prediction in these two breast regions has poor performance. According to the *MAE* of the PSO-BP model, the left breasts have better prediction accuracy than the right breasts. Therefore, it is more effective to predict the left breast motions based on the gait parameters. The result might be related to the stretch ranges and the dispersion of the breast motions.

Discussion

The awareness of breast motion patterns is significant to the optimization of bra comfort and support. A scientific and reasonable parameter utilized to quantify breast motions makes the results more comprehensive and reliable. Numerous reports have described the breast motions based on the points (Scurr et al., 2010; Zhou et al., 2009), but these studies were unable to reflect the motions of the breast regions. Herein, the distance alteration between breast points (Δd) was utilized to analyze the breast motions. The indicator aims to explore the line variation of different breast regions and it reflects the extension and contraction of breast regions. In this study, the results reveal that the main breast motions are the extension. Whether the same breast regions on the different sides of the breasts, or the various breast regions on the same side of the breasts, they all present a significant diversity in breast motions. The phenomenon may be related to the asymmetrical mass of the breasts. There are no consistent results for the motion intensity in different breast regions, and the motions in the right breasts show relatively larger fluctuation than that in the left breasts. The breast displacement of females varies mainly in the vertical direction during the two-step jumping exercise, and the vertical displacement accounts for 58% of the breast displacements (Bridgman et al., 2010). When females exercise on a treadmill at 10 km/h, the vertical, mediolateral, and anteroposterior components account for an average of 56%, 22%, and 19% of breast motions, respectively (Zhou et al., 2012). However, there is a dissimilar result for the breast motions in this study. The breast motions obtain maximum and minimum values in the d_{01} and d_{03} regions respectively, which demonstrates that the motions are more active in the lateral breast areas, followed by the vertical breast areas. Meanwhile, the medial breast areas present the slightest motions. The discrepancies with previous reports may be due to the different indicators of breast motions.

As for the breast motions and the trunk movements, some reports claimed that they all present a pattern of the sinusoidal curve (Haake & Scurr, 2010). However, the foot height off the ground is the only parameter founded in this study that shows a sinusoidal curve with time. The rotation angles of the lower limb joints and the distance alterations of the breast regions all show a 'W' shape during a gait cycle. It is interesting to note that the breast regions exhibit a 'rebound' phenomenon during exercises. In research of dynamic model for the breasts, the 'double bounce' phenomenon was also observed at the minimum value of the breast motion curves (Haake & Scurr, 2010), and the researchers suggested that this phenomenon might be related to the dynamic forces of heel and forefoot strike during contact. Besides, there is a time delay between the curves of certain breast areas and that of limb rotation angles. The phenomenon is also discovered in the study investigating the absolute and relative displacement of breasts during walking and running (Scurr et al., 2009). In the report, both the vertical and resultant breast displacements show a 'bimodal distribution' within a single gait cycle and the peaks and troughs of breast motion curves lag slightly behind the temporal division of the gaits. Once the subject's heel hits the ground during running, that is, at the lowest point where the foot is high off the ground, the trunk suddenly decelerates and falls vertically. Nevertheless, the soft tissue of the breasts continues to move downward due to the inertia, and the breasts only begin to decelerate when the trunk starts to move upward (McGhee et al.,

2010). The time delay in trunk-breast motions causes the breasts to slap down against the chest wall and thus leads to the breast pain (Scurr et al., 2009; McGhee et al. 2013).

According to this analysis, there is a moderate correlation between breast motions and gaits. Thus, the BP neural network, the PSO, and the GA algorithms were applied in this study to develop three prediction models for breast motions. The R^2 of these three models reaches more than 80%, and the PSO-BP model obtains the maximum R^2 of 84.58%. Meanwhile, the PSO-BP model also has the smallest overall *MAE* of 0.2108. Therefore, the PSO-BP algorithm is considered to be more appropriate for breast motion prediction in this study. The validity of the prediction model allows researchers to predict breast motions with gait parameters, and the method can facilitate the investigation of breast motions in different environments lacking the access to measure the breast motions.

There are some limitations in this study, such as the correlation between breast motions and human gaits is only investigated under the bare breasts. For further research, it is vital to explore the difference of breast motions between the bare breasts and the bra-wearing breasts. Furthermore, the influence of bra structures, fabrics, and styles for the breast motions should also be analyzed to reduce breast expansion and contraction during exercises. Besides, the methods in this study are also applicable to investigate the breast motions for other subjects. The awareness of breast motions among different females in a series of exercises is helpful to improve bra support and comfort.

Conclusions

In this study, the distance alteration of the breast regions (Δd) was determined to evaluate breast motions. According to the analysis of the breast motions, a significant motion difference appears in the same regions on the bilateral breasts and the different regions on the ipsilateral breasts. Meanwhile, the Δd-time curves of eight breast regions show the same continuous 'V' pattern. Within a gait cycle, four gait parameters (the hip, the knee, the ankle joint rotation angles, and the foot height off the ground) demonstrate one period while breast motions present two periods. At the same time, the curves of the hip, the knee, the ankle joint rotation angles, and the Δd perform one peak and two troughs respectively. However, there is a slight difference in the occurred time of peaks and troughs. In this case, there is a moderate correlation between breast motion indicators and gait parameters in this study. Therefore, the BP neural network combined with optimization algorithms (the GA and PSO algorithms) is valid to predict breast motions based on gait parameters. Among these three models, the PSO-BP algorithm has the highest prediction accuracy which has an R^2 of 84.58% and an *MAE* of 0.2108.

Acknowledgements
Not applicable.

Authors' contributions
ZHOU J, MQ were responsible for the experiment design and whole structure construction, while MQ, ZHANG J and L.M.L.N was responsible for the data collection, data cleaning, and MQ was responsible for data processing and modelling. The manuscript drafted by MQ and ZHOU J, finally revised by CJM, ZHANG J, L.M.L.N, MQ, ZHOU J. All authors read and approved the final manuscript.

Author's information
Jie ZHOU, Professor, School of Apparel and Art Design, Xi'an Polytechnic University, No. 19 Jinhua South Road, Xi'an, Shaanxi, China. Qian MAO, Master Student, School of Apparel and Art Design, Xi'an Polytechnic University, No. 19 Jinhua South Road, Xi'an, Shaanxi, China. Jun ZHANG, PhD Student, School of Design, The Hong Kong Polytechnic University,

Hung Hom, Kowloon, Hong Kong. Newman M.L.LAU, Associate Professor, School of Design, The Hong Kong Polytechnic University, Hung Hom, Kowloon, Hong Kong. Jianming CHEN, Department of Biomedical Engineering, The Chinese University of Hong Kong, Shatin, New Territories, Hong Kong.

Funding
This work was supported by Shaanxi Science and Technology Department International Science Technology Cooperation Funding (Grant Number 2018KW-056).

Availability of data and materials
The datasets used and/or analyzed during the current study are available from the corresponding author on reasonable request.

Declarations

Competing interests
The authors declare that they have no competing interests.

Ethics declarations
This research was conducted under the exemption and supervision of The Hong Kong Polytechnic University Institutional Review Board(IRB Exemption No. HSEARS20200205001) regarding ethical issues.

Author details
[1]School of Apparel and Art Design, Xi'an Polytechnic University, No. 19 Jinhua South Road, Xi'an, Shaanxi, China. [2]School of Design, The Hong Kong Polytechnic University, Hung Hom, Kowloon, Hong Kong. [3]Department of Biomedical Engineering, The Chinese University of Hong Kong, Shatin, New Territories, Hong Kong.

Received: 29 January 2021 Accepted: 27 October 2021
Published online: 25 January 2022

References

Boyd, N., Martin, L., Chavez, S., Gunasekara, A., Salleh, A., Melnichouk, O., Yaffe, M., Friedenreich, C., Minkin, S., & Bronskill, M. (2009). Breast-tissue composition and other risk factors for breast cancer in young women: A cross-sectional study. *The Lancet Oncology, 10*(6), 569–580. https://doi.org/10.1016/S1470-2045(09)70078-6

Bridgman, C., Scurr, J., White, J., Hedger, W., & Galbraith, H. (2010). Three-dimensional kinematics of the breast during a two-step star jump. *Journal of Applied Biomechanics, 26*(4), 465–472. https://doi.org/10.1123/jab.26.4.465

Cai, Y., Chen, L., Yu, W., Zhou, J., Wan, F., Suh, M., & Chow, D. H. K. (2018). A piecewise mass-spring-damper model of the human breast. *Journal of Biomechanics, 67,* 137–143. https://doi.org/10.1016/j.jbiomech.2017.11.027

Coltman, C. E., Steele, J. R., & McGhee, D. E. (2017). Effect of aging on breast skin thickness and elasticity: Implications for breast support. *Skin Research and Technology, 23*(3), 303–311. https://doi.org/10.1111/srt.12335

Den Tonkelaar, I., Peeters, P. H. M., & Van Noord, P. A. H. (2004). Increase in breast size after menopause: Prevalence and determinants. *Maturitas, 48*(1), 51–57. https://doi.org/10.1016/j.maturitas.2003.10.002

Ding, F. J., Jia, X. D., Hong, T. J., & Xu, Y. L. (2020). Flow stress prediction model of 6061 aluminum alloy sheet based on GA-BP and PSO-BP neural networks. *Rare Metal Materials and Engineering, 49*(6), 1840–1853. https://chn.oversea.cnki.net/kcms/detail/detail.aspx?FileName=COSE202006003&DbName=CJFQ2020

Eden, K. B., Valiant, G. A., Lawson, L. J., & Himmelsbach, J. (1992). Three dimensional kinematic evaluation of sport bra design: 1121. *Medicine & Science in Sports & Exercise, 24*(5), 187. https://doi.org/10.1249/00005768-199205001-01122

Gehlsen, G., & Albohm, M. (1980). Evaluation of sports bras. *The Physician and Sportsmedicine, 8*(10), 88–97. https://doi.org/10.1080/00913847.1980.11948653

Haake, S., & Scurr, J. (2010). A dynamic model of the breast during exercise. *Sports Engineering, 12*(4), 189–197. https://doi.org/10.1007/s12283-010-0046-z

Huang, S. Y., Boone, J. M., Yang, K., Packard, N. J., McKenney, S. E., Prionas, N. D., Lindfors, K. K., & Yaffe, M. J. (2011). The characterization of breast anatomical metrics using dedicated breast CT. *Medical Physics, 38*(4), 2180–2191. https://doi.org/10.1118/1.3567147

Jin, S. F., Lin, Q. Q., Ma, Q. R., & Zhang, H. (2020). Method for detecting fluff quality of fabric surface based on BP neural network. *Journal of Textile Research, 41*(2), 69–76. https://doi.org/10.13475/j.fzxb.20181201008

Lee, N. A., Rusinek, H., Weinreb, J., Chandra, R., Toth, H., Singer, C., & Newstead, G. (1997). Fatty and fibroglandular tissue volumes in the breasts of women 20–83 years old: Comparison of X-ray mammography and computer-assisted MR imaging. *American Journal of Roentgenology, 168*(2), 501–506. https://doi.org/10.2214/ajr.168.2.9016235

Li, S. X., Ren, J. P., & Zhou, X. L. (2018). Influence of sports bra on breast kinematic characteristics and the gait parameters under different stride frequencies. *Journal of Beijing Sport University, 41*(1), 82–88. https://doi.org/10.19582/j.cnki.11-3785/g8.2018.01.012

Liang, S. Z., Zhang, X., & Zhou, J. (2007). Basic breast shapes of female undergraduate in the west of China based on 3-D body scanning. *Journal of Textile Research, 28*(8), 75–78. https://doi.org/10.13475/j.fzxb.2007.08.020

Lorentzen, D., & Lawson, L. (1987). Selected sports bras: A biomechanical analysis of breast motion while jogging. *The Physician and Sportsmedicine, 15*(5), 128–139. https://doi.org/10.1080/00913847.1987.11709355

Losken, A., Fishman, I., Denson, D. D., Moyer, H. R., & Carlson, G. W. (2005). An objective evaluation of breast symmetry and shape differences using 3-dimensional images. *Annals of Plastic Surgery, 55*(6), 571–575. https://doi.org/10.1097/01.sap.0000185459.49434.5f

Mao, Q., Zhou, J., & Wang, Q. (2020). Breast shape recognition of young women in the west of China based on GRNN and PNN. *Journal of Xi'an Polytechnic University, 34*(04), 7–13. https://doi.org/10.13338/j.issn.1674-649x.2020.04.002
Mason, B. R., Page, K. A., & Fallon, K. (1999). An analysis of movement and discomfort of the female breast during exercise and the effects of breast support in three cases. *Journal of Science and Medicine in Sport, 2*(2), 134–144. https://doi.org/10.1016/S1440-2440(99)80193-5
McGhee, D. E., Power, B. M., & Steele, J. R. (2007). Does deep water running reduce exercise-induced breast discomfort? *British Journal of Sports Medicine, 41*(12), 879–883. https://doi.org/10.1136/bjsm.2007.036251
McGhee, D. E., & Steele, J. R. (2020a). Breast biomechanics: What do we really know? *Physiology, 35*(2), 144–156. https://doi.org/10.1152/physiol.00024.2019
McGhee, D. E., & Steele, J. R. (2020b). Biomechanics of breast support for active women. *Exercise and Sport Sciences Reviews, 48*(3), 99–109. https://doi.org/10.1249/JES.0000000000000221
McGhee, D. E., Steele, J. R., & Munro, B. J. (2010). Education improves bra knowledge and fit, and level of breast support in adolescent female athletes: A cluster-randomised trial. *Journal of Physiotherapy, 56*(1), 19–24. https://doi.org/10.1016/s1836-9553(10)70050-3
McGhee, D. E., Steele, J. R., Zealey, W. J., & Takacs, G. J. (2013). Bra–breast forces generated in women with large breasts while standing and during treadmill running: Implications for sports bra design. *Applied Ergonomics, 44*(1), 112–118. https://doi.org/10.1016/j.apergo.2012.05.006
Milligan, A., Mills, C., Corbett, J., & Scurr, J. (2015). The influence of breast support on torso, pelvis and arm kinematics during a five kilometer treadmill run. *Human Movement Science, 42*, 246–260. https://doi.org/10.1016/j.humov.2015.05.008
Pei, J., Fan, J., & Ashdown, S. P. (2019). A novel method to assess breast shape and breast asymmetry. *The Journal of the Textile Institute, 110*(8), 1229–1240. https://doi.org/10.1080/00405000.2018.1555876
Prakash, C., Kumar, R., & Mittal, N. (2018). Recent developments in human gait research: Parameters, approaches, applications, machine learning techniques, datasets and challenges. *Artificial Intelligence Review, 49*(1), 1–40. https://doi.org/10.1007/s10462-016-9514-6
Ren, J. P., Sun, M. Z., Zhou, X. L., & Zhang, J. (2016). Research on the asymmetry of the left and right breast during walking. *Journal of Capital University of Physical Education and Sports, 28*(04), 360–364. https://doi.org/10.14036/j.cnki.cn11-4513.2016.04.016
Ren, J. P., Yan, Y., & Zhou, X. L. (2015). Research on the impact of sports bras on breast movements in walking and running with different speeds. *Journal of Capital University of Physical Education and Sports, 27*(02), 172–177. https://doi.org/10.14036/j.cnki.cn11-4513.2015.02.016
Scurr, J., White, J., & Hedger, W. (2009). Breast displacement in three dimensions during the walking and running gait cycles. *Journal of Applied Biomechanics, 25*(4), 322–329. https://doi.org/10.1123/jab.25.4.322
Scurr, J. C., White, J. L., & Hedger, W. (2010). The effect of breast support on the kinematics of the breast during the running gait cycle. *Journal of Sports Sciences, 28*(10), 1103–1109. https://doi.org/10.1080/02640414.2010.497542
Scurr, J. C., White, J. L., & Hedger, W. (2011). Supported and unsupported breast displacement in three dimensions across treadmill activity levels. *Journal of Sports Sciences, 29*(1), 55–61. https://doi.org/10.1080/02640414.2010.521944
Shen, X. J., Fu, X. J., & Zhou, C. C. (2018). Characteristics of outliers in wind speed-power operation data of wind turbines and its cleaning method. *Transactions of China Electrotechnical Society, 33*(14), 3353–3361. https://doi.org/10.19595/j.cnki.1000-6753.tces.171129
Wang, H. L., Zhu, Y. A., Xu, W. W., Xu, R., Huang, Y. G., & Lu, W. (2019). Extraction and importance ranking of features for gait recognition. *Chinese Journal of Medical Physics, 36*(07), 811–817. https://oversea.cnki.net/kns/detail/detail.aspx?FileName=YXWZ201907013&DbName=CJFQ2019
White, J. L., Scurr, J. C., & Smith, N. A. (2009). The effect of breast support on kinetics during overground running performance. *Ergonomics, 52*(4), 492–498. https://doi.org/10.1080/00140130802707907
Wood, L. E., White, J., Milligan, A., Ayres, B., Hedger, W., & Scurr, J. (2012). Predictors of three-dimensional breast kinematics during bare-breasted running. *Medicine and Science in Sports and Exercise, 44*(7), 1351–1357. https://doi.org/10.1249/MSS.0b013e31824bd62c
Xiao, X. P. (1997). Theoretical study and reviews on the computation method of grey interconnet degree. *Systems Engineering-Theory & Practice, 8*, 77–82. https://doi.org/10.12011/1000-6788(1997)8-77
Zhang, J., & Guo, W. H. (2019). Research on railway passenger flow prediction method based on GA improved BP neural network. *Journal of Computer and Communications, 7*(7), 283–292. https://chn.oversea.cnki.net/kcms/detail/detail.aspx?FileName=MGKY201907001002&DbName=IPFD2019
Zhou, J., & Ma, Q. R. (2019). Prediction of relationship between shoulder strap attribute and breast amplitude of sports bra by BP neural network. *Journal of Textile Research, 40*(9), 186–191. https://doi.org/10.13475/j.fzxb.20181001406
Zhou, J., & Ma, Q. R. (2020). Establishing a genetic algorithm-back propagation model to predict the pressure of girdles and to determine the model function. *Textile Research Journal, 90*(21–22), 2564–2578. https://doi.org/10.1177/0040517520922947
Zhou, J., Yu, W., & Ng, S. P. (2012). Studies of three-dimensional trajectories of breast movement for better bra design. *Textile Research Journal, 82*(3), 242–254. https://doi.org/10.1177/0040517511435004
Zhou, J., Yu, W., Ng, S. P., & Hale, J. (2009). Evaluation of shock absorbing performance of sports bras. *Journal of Fiber Bioengineering and Informatics, 2*(2), 108–113. https://doi.org/10.3993/jfbi09200906

Publisher's Note